Published in final edited form as:

J Cell Physiol. 2017 June ; 232(6): 1306–1317. doi:10.1002/jcp.25599.

A MicroRNA Cluster miR-23–24–27 Is Upregulated by Aldosterone in the Distal Kidney Nephron Where it Alters Sodium Transport

XIAONING LIU[1], **ROBERT S. EDINGER**[1], **CHRISTINE A. KLEMENS**[1], **YU L. PHUA**[2], **ANDREW J. BODNAR**[2], **WILLIAM A. LAFRAMBOISE**[3], **JACQUELINE HO**[2], and **MICHAEL B. BUTTERWORTH**[1,*]

[1]Department of Cell Biology, University of Pittsburgh School of Medicine, Pittsburgh, Pennsylvania

[2]Division of Nephrology in the Department of Pediatrics, University of Pittsburgh School of Medicine, Pittsburgh, Pennsylvania

[3]Department of Pathology, University of Pittsburgh School of Medicine, Pittsburgh, Pennsylvania

Abstract

The epithelial sodium channel (ENaC) is expressed in the epithelial cells of the distal convoluted tubules, connecting tubules, and cortical collecting duct (CCD) in the kidney nephron. Under the regulation of the steroid hormone aldosterone, ENaC is a major determinant of sodium (Na^+) and water balance. The ability of aldosterone to regulate microRNAs (miRs) in the kidney has recently been realized, but the role of miRs in Na^+ regulation has not been well established. Here we demonstrate that expression of a miR cluster mmu-miR-23–24–27, is upregulated in the CCD by aldosterone stimulation both in vitro and in vivo. Increasing the expression of these miRs increased Na^+ transport in the absence of aldosterone stimulation. Potential miR targets were evaluated and miR-27a/b was verified to bind to the 3′-untranslated region of intersectin-2, a multi-domain protein expressed in the distal kidney nephron and involved in the regulation of membrane trafficking. Expression of Itsn2 mRNA and protein was decreased after aldosterone stimulation. Depletion of Itsn2 expression, mimicking aldosterone regulation, increased ENaC-mediated Na^+ transport, while Itsn2 overexpression reduced ENaC's function. These findings reinforce a role for miRs in aldosterone regulation of Na^+ transport, and implicate miR-27 in aldosterone's action via a novel target.

Short, non-coding RNAs termed microRNAs (miRs) bind predominantly to the untranslated regions (UTRs) of target mRNAs to decrease target protein expression (Lewis et al., 2003, 2005; Abbott et al., 2005). In the kidney, miRs have been shown to regulate or be involved in kidney development (Ho et al., 2008, 2011; Agrawal et al., 2009; Pastorelli et al., 2009; Chu et al., 2014), kidney cancers (Abdelmohsen et al., 2010; Powers et al., 2011; Wei et al.,

*Correspondence to: Michael B. Butterworth, Department of Cell Biology, University of Pittsburgh School of Medicine, S314 BST, 200 Lothrop St Pittsburgh, PA 15261. michael7@pitt.edu.

Xiaoning Liu and Robert S. Edinger contributed equally to the study.

Supporting Information

Additional supporting information may be found in the online version of this article at the publisher's web-site.

2013), diabetic nephropathy (Kato et al., 2007, 2010; Krupa et al., 2010), polycystic kidney disease (Pandey et al., 2008, 2011), fibrotic kidney disease (Kato et al., 2009; Krupa et al., 2010; Qin et al., 2011; Zhong et al., 2011), and acute kidney injury (Harvey et al., 2008; Ho et al., 2008; Shi et al., 2008; Wei et al., 2010; Lorenzen et al., 2011). miRs also play a significant role in kidney maintenance and normal kidney physiology (Sequeira-Lopez et al., 2010; Mladinov et al., 2013). Recent evidence suggests that miRs may be important intermediaries in the hormonal signaling cascades that alter ion transport in both the airway (Qi et al., 2015; Qin et al., 2016) and the kidney (Elvira-Matelot et al., 2010; Sober et al., 2010; Robertson et al., 2013; Edinger et al., 2014; Butterworth, 2015; Jacobs et al., 2016).

The mineralocorticoid hormone aldosterone is released from the adrenal glands as the final signaling product of the renin-angiotensin-aldosterone system (RAAS) in a homeostatic response to decreased plasma sodium (Na^+) levels or reduced plasma volume (Pacha et al., 1993; Loffing et al., 2001). The renal consequence of increased circulating aldosterone levels is an increase in Na^+ reabsorption in the kidney distal nephron, predominantly through an increase in the activity of Na^+ transporters in these distal nephron segments (Verrey, 1995; Asher et al., 1996). This in turn increases Na^+ and osmotic water reabsorption to regulate plasma fluid volume and therefore blood pressure (Campese and Park, 2006; Hsueh and Wyne, 2011). Aldosterone binds to the mineralocorticoid receptor (MR) which initiates translocation of the MR complex to the nucleus, where it interacts with mineralocorticoid response elements (MREs) found within the promoter region of hormone-induced genes including miRs, to alter gene expression. In the principal cells, of the kidney cortical collecting duct (CCD) aldosterone modulates the expression of a number of proteins, including the epithelial sodium channel (ENaC), that ultimately lead to an increase in Na^+ uptake (Muller et al., 2003; McCormick et al., 2005; Martel et al., 2007). Aldosterone exhibits differential regulation of targets in different epithelia, suggesting the possibility that MREs are differentially targeted, or that there is an additional intermediate regulatory step in the MR signaling cascade (Spindler et al., 1997; Verrey et al., 2007). One such intermediate is miR regulation. While miRs differ significantly in their tissue distribution (Farh et al., 2005; Landgraf et al., 2007), we previously demonstrated that aldosterone regulates miRs in CCD principal cells with the change in expression of at least 20 miRs including the upregulated miRs investigated in this study (Edinger et al., 2014). Our previous work reported on the roles of the downregulated miRs in Na^+ regulation, but no information is currently available describing a role for the miRs that are induced by aldosterone in the distal kidney nephron, or the impact of these aldosterone-induced miRs on Na^+ transport in the kidney. While we observed a number of miRs whose expression was increased in response to aldosterone, two miR clusters were coordinately induced and comprise the members of the miR-23–24–27 family. Exogenous overexpression of miR-27 in mCCD cells increased the activity of the epithelial sodium channel (ENaC) in the absence of aldosterone stimulation. In silico target prediction provided a number of possible miR-27 target proteins which were screened in a mouse CCD (mCCD) cell line, including intersectin-2 (Itsn2). Itsn2 is regulated by both a change in miR-27 levels, or with aldosterone stimulation. Changes in Itsn2 expression were able to alter ENaC function and Na^+ transport in mCCD cells. This study reinforces an important role for miRs as a new element in the RAAS signaling cascade that maintains Na^+ transport in the kidney.

Materials and Methods

Antibodies and reagents

All chemicals were purchased from Sigma–Aldrich (St. Louis, MO) or Thermo Fisher (Pittsburgh, PA) unless noted otherwise. Antibodies used are as follows: anti-Dicer (rabbit polyclonal, Biovision, San Francisco, CA), anti-β-Actin (mouse, monoclonal, Sigma–Aldrich), anti- Itsn2 (goat polyclonal, Santa Cruz Biotechnology, Santa Cruz, CA and rabbit polyclonal, Novus Biologicals, Littleton, CO), GFP (Rabbit polyclonal, Invitrogen/Thermo Fisher, Carlsbad, CA), and Aqp2 (rabbit, polyclonal, Calbiochem cat #KP9201, now EMD Millipore, Temecula, CA).

Mice and metabolic experiments

C57Bl/6 2-month-old mice (n = 8) (obtained from Charles River Laboratories, Wilmington, MA) were fed in their home cage with standard diet (0.25% sodium) for 7 days, and were placed in metabolic cages for two 24 h periods to determine water and food consumption, urine and feces excretion, and collect urine. These mice were then switched to a low salt diet (0.01–0.02% sodium, Sodium Deficient Diet, Harlan, Frederick, MD) for 7 days, and placed in metabolic cages for two 24 h periods to monitor the same metabolic parameters a described before (Edinger et al., 2014). Kidneys and blood samples were collected from the animals. An equal number of animals were fed with a low salt diet first for 7 days, placed in metabolic cages for twice for 24 h, switched to standard diet for 7 days, and then placed in metabolic cages for twice for 24 h. Urine (n = 8 for each group) and plasma (n = 4 for each group) samples were sent to Kansas State University Veterinary Diagnostic Laboratories, Clinical Pathology Laboratory (Manhattan, KS) to determine urine and plasma electrolytes and osmolality. All animals were housed in the vivarium at Rangos Research Center at Children's Hospital of Pittsburgh of UPMC, Pittsburgh, PA, and all animal experiments were carried out in accordance with the policies of the Institutional Animal Care and Use Committee at the University of Pittsburgh.

Cell culture

The mCCDc11 cells (kindly provided by B. Rossier and L. Schild, Université de Lausanne, Lausanne, Switzerland) were grown in flasks (passages 30–40) in defined (supplemented) medium at 37°C in 5% CO_2 as described previously (Edinger et al., 2012, 2014). The medium was changed every 2nd day. For electrophysiological experiments, the mCCD cells were subcultured onto permeable filter supports (0.4 μm pore size, 0.33 or 4 cm^2 surface area; Transwell, Corning, Lowell, MA). Typically, 24 h before use in any investigation, medium incubating filter-grown cells was replaced with a minimal medium (without drugs or hormones) that contained DMEM and Ham F12 only. HEK-293 cells (from ATCC) were grown in flasks in DMEM (Invitrogen) supplemented with 10% FCS.

Plasmid construction

The 3′ UTR of Itsn2 was obtained from cDNA clone IMAGE:4506047. Primer pairs containing a sequence-specific primer (5′ TCTCGAGGGCCTGGGGAAGCCAGAAC-3′ forward) which incorporated a XhoI site at the 5′ end and a vector specific primer T7

(reverse) were used to amplify the UTR which was sub-cloned into pCR-blunt (Invitrogen). The resulting 906bp UTR represents the 3′ UTR starting with the nucleotide after the termination codon of Itsn2 and extending to the beginning of the polyadenylation tail. The resulting construct was digested with XhoI and NotI restriction endonucleases to release the 3 UTR. The fragment was cloned into the XhoI/NotI restriction sites of pMir-Glo. The putative miR-27 site, located at position575–596 bp away from theterminationcodon, was mutated by PCR to eliminate the site. The sequences for the mutagenesis were as follows 5′ fragment (5′-GAGAATTCATCAAGCTTTCCTCCTTATATTC-3′ forward and 5′-GCAAGATCGCCGTGTAA TTCTAG-3′ reverse); and 3′ fragment (5′-GCGTAAGGAGAAAATACCGCATC-3′ forward and 5′-CAGAATTCTCTAATAATGTGGGGATATTTTTCAAC-3′ reverse). The fragments were digested with EcoRI and ligated using T4 DNA ligase (New England Biolabs, Ipswich, MA). The resulting fragment was digested with XhoI/NotI and cloned into the XhoI/NotI restriction sites of pMir-Glo. All constructs were sequenced (GeneWiz, South Plainfield, NJ) to verify constructs and deletions.

Immunofluorescence imaging

Kidneys collected from standard and low salt diet treated mice were fixed with paraformaldehyde buffer (4% in PBS at pH of 7.4) overnight at 4°C, cryoprotected with 30% sucrose/PBS overnight at 4°C, and embedded in O.C.T (Scigen, Gardena, CA) for cryosectioning. Eight micrometer cryosections used for the co-immunofluorescence were permeabilized with PBS containing 0.1% Tween20 for 5 min, blocked with 1%BSA in PBS containing 0.05% Tween20 for 30 min and incubated with primary anti-Itsn2 antibody and primary anti-Aqp2 (1:100) overnight at 4°C in block buffer. Sections were washed three times with PBS containing 0.05% Tween20 and incubated with secondary antibodies (1:200, Alexa-488 and Alexa-594; Jackson ImmunoResearch) in block buffer for 1 h at room temperature. Following a final PBS + Tween20 wash (three times), nuclei were counterstained using DAPI and mounted with coverslip using Fluorogel (Electron Microscopy Sciences). Images were acquired with a Leica DM2500 microscope equipped with a Qimaging QICAM Fast 1394 camera.

CCD cells treated with or without aldosterone (50 nM, 24 h) were fixed in a cold (4°C) paraformaldehyde buffer (4% in PBS at pH of 7.4). Following 45 min of fixation at 4°C, cells were washed in cold PBS with 1 mM calcium and 0.5 mM magnesium (+CM) three times, and permeabilized in PBS containing 0.1% Triton-X and 0.1% NP-40. Cells were incubated with primary anti–Itsn2 antibody (goat antibody at 1:50 dilution) for 12 h in PBS with 10% skim milk at 4°C. Cells were washed three times in PBS + CM and incubated with a secondary antibody (1:1000, Alexa-488; and Alexa-568 tagged phalloidin; Invitrogen) for 3 h at 37°C. Following a final PBS + CM wash (three times), nuclei were counterstained using 10 nM Hoechst 33342 (Trihydrochloride; Invitrogen). Cells were washed in PBS + CM (three times) and mounted onto slides using Fluoromount-G (Southern Biotech, Birmingham, AL) for imaging, as previously described (Edinger et al., 2014). Images were captured using a Nikon A1 confocal microscope using a Plan Apo VC60×, 1.4 numerical aperture oil objective and Nikon Elements AR software (Nikon, Tokyo, Japan) at the

University of Pittsburgh Center or Biologic Imaging. Linear adjustments of brightness and contrast were made offline in MetaMorph (Molecular Devices, Sunnyvale, CA).

Short-circuit current recordings

Inserts were mounted in modified Ussing chambers (P2300; Physiologic Instruments, San Diego, CA) and continuously short circuited with an automatic voltage clamp (VCC MC8; Physiologic Instruments) as described previously (Edinger et al., 2012, 2014). The apical and basolateral chambers each contained 4 ml of Ringer solution (120 mM NaCl, 25 mM $NaHCO_3$, 3.3 mM KH_2PO_4, 0.8 mM K_2HPO_4, 1.2 mM $MgCl_2$, 1.2 mM $CaCl_2$, and 10 mM glucose). Chambers were constantly gassed with a mixture of 95% O_2, 5% CO_2 at 37°C, which maintained the pH at 7.4 and established a circulating perfusion bath within the Ussing chamber. Simultaneous transepithelial resistance was recorded by applying a 2-mV pulse per minute via an automated pulse generator. Recordings were digitized and analyzed using PowerLab (AD Instruments, Colorado Springs, CO).

Transfections: RNA interference, miRNA overexpression, and depletion

A number of DNA plasmids and RNA oligonucleotide constructs were transiently transfected into the mCCD and HEK293 cells using Lipofectamine 2000 (Invitrogen) according to the manufacturer's instructions and as described previously (Edinger et al., 2012, 2014). The sequences for siRNA and all primers are listed in Supplemental Table S1. Double-stranded RNA miR mimics (miRIDIAN microRNA Mimics) were obtained from Thermo Fisher Scientific. To assay mimic delivery and transfection efficiency, non-targeting, fluorescently labeled control mimics were used (Thermo Fisher Scientific). To inhibit processing to mature miRs and reduce endogenous miR expression, LNA oligonucleotides targeting the miRs along with non-targeting LNA controls were obtained from Exiqon, Inc. (Woburn, MA).

Dual luciferase assays

HEK cells were transfected with pMIR-Glo containing Itsn2 wt or mutant 3′ UTR with or without miR mimics as described above. The following day the cells were sub cultured to a white 96-well plate (Falcon, Thermo Fisher) and returned to the incubator. After 24 h, luciferase activity was determined using the Dual-Glo Luciferase Assay System (Promega, Madison, WI) according to the manufacturer's protocol. Bioluminescence activity was recorded as an endpoint assay on a Synergy 1H plate reader (BioTek Instruments, Winooski, VT), with an integration time of 100 ms at a sensitivity of 200. The same plasmids were transfected in mCCD cells alone, or with miR-27a mimics (as above). Dual luciferase assays of mCCD cells on filters were carried out in 24-well plates as described before (Edinger et al., 2014).

RNA isolation and microarray analysis

RNA from cultured or primary CCD cells was isolated using the miRNeasy RNA isolation kit (Qiagen, Germantown, MD) according to the manufacturer's protocol. The kit facilitated isolation of both miRNA and total RNA from each sample for use in qRT-PCR, RT-PCR, and microarray analysis. Total RNA (containing miRNAs) concentration and quality were

evaluated for inclusion in subsequent in vitro transcription assays based on a spectrophotometric absorption ratio of 260/280 >1.8 (NanoDrop, Wilmington, DE) and an RIN (RNA integrity number) value of >5.0 via electrophoretic analysis (Agilent Bioanalyzer 2100; Agilent Technologies, Santa Clara, CA). Direct labeling of the miRNA using the Exiqon miRCURY LNA Hy3 Power Labeling Kit (Exiqon, Inc.) was performed on five paired expansions of mCCD cells cultured under standard conditions (n = 5) or after 24 h of 50 nM aldosterone treatment (n = 5) as described previously (Edinger et al., 2014). Briefly, 1 μg of total RNA from each sample was incubated with Calf Intestinal Phosphatase (4 μl reaction volume) at 37°C for 30 min in an Eppendorf Thermostat Plus heat block (Eppendorf Inc., Hauppauge, NY). The samples were then denatured at 95°C for 5 min. Labeling Enzyme and Hy3 fluorescent label (Exiqon, Inc.) were added to each sample (12.5 μl final volume) for incubation at 16°C for 1 h, followed by 15 min at 65°C. Hybridization buffer was added to each sample to a 400 μl volume, followed by denaturation at 95°C for 2 min before manual hybridization on Exiqon miRCURY LNA HSA, MMU, RNO spotted nucleotide arrays (Homo sapiens, Mus musculus, and Rattus norvegicus). For each sample, an Agilent gasket slide (one microarray per slide format, part #G2534–60003; Agilent Technologies) was placed in an Agilent hybridization chamber and the entire sample was pipetted onto the gasket slide. The Exiqon array was then placed onto the gasket slide with the probe side facing down. The loaded hybridization chambers were clamped closed and placed into the hybridization oven for overnight incubation (18 h at 56°C and 20 rpm).

The arrays were manually washed using CodeLink Parallel Processing Kits (Applied Microarrays Inc., Tempe, AZ) with Exiqon miRCURY LNA array Washing Buffer Kit (Exiqon, Inc.) according to the manufacturer's specifications. The arrays were scanned on an Axon GenePix 4000 B scanner (Molecular Devices Inc., Sunnyvale, CA) (settings: pixel size, 5 μm, 635 photomultiplier tube 600, 635 power 100, 532 photomultiplier tube 650, 532 power 100) and analyzed using GenePix Pro 6.0 software (Molecular Devices Inc.) with annotation of sequences from Sanger miRBase version 11.0. Local background subtraction was applied to each probe before averaging target replicates, and these values were compared with a threshold value determined from "negative" probes distributed throughout the array. Data from the 10 arrays were quantile normalized followed by testing for statistical differences using the paired *t*-test function (false discovery rate ≤0.05) in the Significance Analysis of Microarrays software (SAM version 4.0.79).

qRT-PCR

Primers and primer pairs used for all PCRs are listed in Supplemental Table S1. For qRT-PCR of miRNA, the nCode Express SYBR-Green miRNA with ROX qRT-PCR kit was used for reverse transcription and first-strand DNA synthesis (Invitrogen). For all miRNA qPCRs, the miRNA-specific forward primers were paired to a universal reverse primer per the manufacturer's protocol. Real-time PCR was carried out using an Applied Biosystems 7900HT Fast Real-Time PCR System (Applied Biosystems, Life Technologies, Grand Island, NY). Detected signals from miR amplifications were normalized to the relative expression of small nucleolar RNA (SNO-202 and SNO-135) with each reaction/sample run in triplicate. Negative controls included no template and no primer omissions. The standard qPCR protocol is provided in Supplemental Table S1. For qPCR of mRNA, primer pairs

were used as listed (Supplemental Table S1), using the Express SYBR-Green with ROX qPCR kit (Invitrogen). Relative mRNA was normalized to the glyceraldehyde 3-phosphate dehydrogenase or actin message from each sample, and expression is presented as a fold change from control untreated samples (ΔΔCT).

Ex vivo kidney CCD cell isolation

Distal kidney nephron principal epithelial cells were isolated from a crude kidney tubules preparation using a lectin binding and magnetic bead isolation technique as described before (Edinger et al., 2014). The isolated cells were immediately processed for RNA isolation; isolated RNA was used immediately or stored at −80°C until needed.

Western blot

Lysates were prepared in cell lysis buffer (0.4% deoxycholic acid, 1% Nonidet P-40, 50 mM EGTA, 10 mM Tris-Cl, pH 7.4) plus protease inhibitors at 4°C for 10 min. The lysates were heated to 70°C for 5 min, separated by SDS–PAGE, transferred to Immobilon-P (EMD Millipore) and subjected to Western blot analysis using antibodies as indicated.

Blot quantification and statistical analyses

Densitometric quantification of protein band intensities was carried out in Adobe Photoshop CS5.1 (Adobe Systems, Inc., San Jose, CA), and values were expressed as a percentage of control signal, following background subtraction, and normalization to total protein expression (actin). Statistical analyses were performed using GraphPad Prism (Systat, La Jolla, CA). All data are presented as mean ±SEM. Data sets to be compared were tested for equal variance, and comparisons were performed using *t* tests or Mann–Whitney rank-sum tests. Groups were considered statistically significant different at $P < 0.05$.

Results

Aldosterone increases miR cluster expression in mCCD cells

To determine which miRs may be upregulated by aldosterone in the distal kidney nephron, mCCD cells cultured on filter supports were stimulated with aldosterone (50 nM) for 24 h and changes in miR expression examined by microarray analysis (Fig. 1A and reported previously (Edinger et al., 2014)). A number of miRs were significantly upregulated, including the miR clusters mmu-miR-23a–24-2–27a (miRC11) and mmu-miR-23b–24-1–27b (miRC22). These clusters are expressed on two separate chromosomes in human (chromosomes 19 and 13) and mouse (chromosomes 8 and 13 in mouse). To verify the array results mCCD cells were treated with aldosterone (24 h, 50 nM) and a qPCR analysis of miR expression confirmed the increase in miR cluster expression (Fig. 1B).

miR clusters are up-regulated in CCD in vivo

To investigate if a similar regulation occurs in principal cells of the collecting duct in vivo, mice of both sexes were placed on low sodium diets to induce aldosterone signaling, as we and others have done previously (Nesterov et al., 2012; Pouly et al., 2013; Edinger et al., 2014). Kidneys were harvested and CCD cells isolated. Quantitative PCR of miRs from

magnetically isolated CCD epithelial cells confirmed the upregulation of these miR clusters in vivo after aldosterone stimulation induced by the low Na^+ diet (Fig. 1C).

miR-27 alters ENaC-mediated Na^+ transport

To test if these miR clusters formed part of an aldosterone signaling cascade responsible for regulating Na^+ transport, miR mimics or inhibitors (locked nucleic acids) of each cluster member were transfected into mCCD cells. The specific change in miR expression in the mCCD cells, either an endogenous depletion with miR inhibitors or an exogenous increase for mimics, was verified by qPCR (Fig. 2A). Amiloride-sensitive short-circuit current (I_{SC}) was recorded in cells overexpressing individual miR cluster member mimics to determine the impact on ENaC activity in the absence of hormonal or serum supplementation. Overexpression of miR-27 increased ENaC-mediated Na^+ transport (Fig. 2B), and no significant increase in ENaC activity was observed with miR-23 or miR-24 mimics (Fig. 2C). For this reason, focus shifted to investigating miR-27a/b regulation of ENaC-mediated Na^+ transport.

Both baseline (Fig. 2B) and aldosterone stimulated (Fig. 2C) ENaC current was higher in cells overexpressing miR-27 (mimic) compared to control, unstimulated cells. However, the response to aldosterone was not significantly higher than control cells stimulated with aldosterone (Fig. 2D). This suggested that aldosterone was signaling through the miRs to alter ENaC activity, rather than in parallel to a miR response. As confirmation of this, selective inhibition of miR-27 using miR inhibitors followed by aldosterone stimulation significantly blunted ENaC's response to aldosterone (Fig. 2D). As a control, overexpression of the non-aldosterone regulated miR-10a, which is abundant in the mCCD cells and in epithelial cells in distal nephron segments in vivo did not alter baseline ENaC activity or the response to aldosterone stimulation (Fig. 2C).

miR-27 is sufficient to transduce aldosterone signaling

To demonstrate a singular role of miR-27 in aldosterone signaling, the miR processing enzyme, Dicer1 was depleted in mCCD to inhibit processing of pre-miRs to fully mature miRs and reduce the formation of miR silencing complexes (Fig. 3A). As we demonstrated previously, with a reduced ability to produce mature miRs, mCCD cells have a significantly blunted response to aldosterone stimulation compared to control transfected cells (Edinger et al., 2014). As a confirmation of these previous findings, depletion of Dicer1 in mCCD cells again produced a significantly smaller response to aldosterone stimulation (Fig. 3B). Concurrent with the Dicer1 depletion, we transfected mature miR mimics into mCCD cells, and then allowed cells to polarize on filter supports before stimulating with aldosterone. Control cells with Dicer depletion alone, or in which the miR-10a was overexpressed as a control, failed to significantly respond to aldosterone (Fig. 3B). Cells with Dicer depletion and miR-27 overexpression were able to respond significantly to aldosterone stimulation and increase ENaC-mediated Na^+ transport (Fig. 3B). By normalizing currents to the control siRNA transfected cells for each replicate, the response to aldosterone for each experimental group could be determined (Fig. 3C). In all cases of Dicer depletion there was a significantly increased I_{SC} relative to unstimulated control (baseline and stimulated I_{SC}). This elevated baseline I_{SC} was only further increased following aldosterone stimulation in cells

overexpressing miR-27 mimic. As there was some variation in baseline currents between experimental days, data were normalized and expressed as a percentage change from the control (unstimulated) current for each group/day (Fig. 3D). The aldosterone stimulation, expressed as a percentage increase over unstimulated cells, was significantly increased in miR-27 overexpressing cells; however, not to the same extent as control cells without Dicer depletion. ENaC-mediated transport in Dicer depleted mCCD cells did not significantly increase after aldosterone stimulation, nor was a significant stimulation observed in Dicer-depleted cells co-transfected with the miR-10a mimic.

miR-27 targets

Potential miR-27 targets were predicted using in silico approaches including TargetScan (Agarwal et al., 2015) and miRDB (Wong and Wang, 2015). To test for possible miR-27 targets, mRNA expression of selected targets was quantified by qPCR from RNA isolated from mCCDs either overexpressing the miR-27a mimic or stimulated with aldosterone (24 h). Results of the limited screen are summarized in Table 1. Candidate targets were considered positive hits if they exhibited downregulation by both miR-27 mimic and aldosterone and these positive hits were then selected for further investigation. One of these screened targets was intersectin 2 (Itsn2). Intersectins have previously been shown to regulate the expression of renal potassium channels in the distal nephron and be regulated by miRs that were altered by changes in K^+ diet in mice, making Itsn2 an ideal candidate for further investigation (Lin et al., 2014).

Immunofluorescent staining of Itsn2 in mouse kidney sections and mCCD cells (Fig. 4) was carried out and images obtained by confocal microscopy. Itsn2 was detected both in distal nephron segments (as determined by co-localization with Aquaporin 2) and in other nephron segments (Fig. 4A). After placing mice on low Na^+ diets the expression of Itsn2 was markedly reduced, including in the Aqp2-positive CCD epithelia (Fig. 4A lower parts). Itsn2 exhibited a punctate/vesicular expression both in vivo and in mCCD cells (Fig. 4B) possibly due to its reported role in endosome formation and the coordination of vesicle trafficking (Pechstein et al., 2010; Tsyba et al., 2011).

Itsn2 expression and regulation by miR-27

Itsn genes (Itsn1 and 2) encode two main protein isoforms consisting of a long isoform (Itsn-L) and a short isoform (Itsn-S) (Tsyba et al., 2011). To determine the isoform found in mCCD cells, specific primers were designed to unique sequences in both isoforms. We confirmed that Itsn2-S is the predominant isoform in the CCD cells (data not shown). This is pertinent as the 3′ UTR in the Itsn-S isoform contains a putative miR-27 site compared to Itsn2-L which lacks any predicted miR-27 binding site.

To confirm that the Itsn2-S UTR was a bona fide miR-27 target, the 3′-UTR was cloned into a dual luciferase reporter construct (pGlo-miR) and transfected into both HEK-293 and mCCD cells for luminescence assays. In addition to the mouse Itsn2 UTR-luciferase construct, a mutant UTR in which the putative miR-27 site was deleted was transfected in HEK293 cells and a dual luciferase assay carried out. Using the two luciferase signals, data were normalized to account for variations in transfection efficiency and then expressed as a

percentage of the control wt-Itsn2-UTR signal alone. Expression of the Itsn2-UTR was significantly decreased when co-transfected with either miR-27a (a perfectly complementary target site) or miR-27b (a single nucleotide mismatch) mimics (Fig. 5A). Several controls were carried out in the HEK293 cells to confirm Itsn2-UTR downregulation by miR-27a and miR-27b. Specifically, no reduction in luciferase signal was observed in the mutant UTR lacking the miR-27 binding site or in wt-Itsn2-UTR co-transfected with miR10a or miR-23a/b and -24, the other members of the miR cluster. These in vitro findings confirmed Itsn2 as a miR-27a/b target as predicted by the in silico analysis.

To determine if the same regulation could be observed in the mCCD cells, the luciferase reporter was transfected into mCCD cells with the miR-27a mimic. Cells were seeded onto filter supports and allowed to polarize before the luciferase assays were carried out on cells grown on filter supports. We noted that in the mCCD cells there was repression of the wt-Itsn2-UTR reporter even before the introduction of miR mimics (Fig. 5B), presumably due to regulation by endogenous miRs present in the mouse cell line. However, when the Itsn2-UTR was co-transfected with miR-27a mimics a further significant reduction in luciferase reporter signal was observed compared to cells expressing the UTR alone, as in the HEK cells (Fig. 5B).

To determine if miR-27 could regulate endogenous Itsn2 protein levels, mCCD cells were transfected with increasing amounts of miR-27 mimic and whole cell expression of Itsn2 determined by Western blot. No change in expression was observed with increased expression of control miR-10a, but a decrease in Itsn2 expression was evident as miR-27 levels increased (Fig. 5C).

Itsn2 is regulated by aldosterone

We next investigated mRNA regulation of Itsn2 by aldosterone signaling. Itsn2 expression was quantitated by PCR in isolated CCD cells from mice on low Na^+ diets compared to mice on normal diets or in mCCD cells stimulated with aldosterone compared to unstimulated controls. In both in vivo and in vitro samples, Itsn2 mRNA expression was reduced by aldosterone signaling (Fig. 6A). As a positive control for aldosterone stimulation, mRNA expression of the well-studied aldosterone-induced protein the serum and glucocorticoid kinase (SGK1) was significantly increased. To demonstrate that this reduction in mRNA signal translated to a change in protein expression, whole-cell protein levels in mCCD cells were determined before and after aldosterone stimulation by Western blot. At 24 h, the Itsn2 protein level was significantly reduced (~55%) compared to unstimulated mCCD cells (Fig. 6B).

Itsn2 alters ENaC-mediated Na^+ transport

To link the change in Itsn2 expression to regulation of ENaC function, Itsn2 protein expression was depleted using siRNA, and mCCD cells seeded to filter supports to measure ENaC transport. Depletion of Itsn2 expression was confirmed by Western blot (Fig. 6C). CCDs in which Itsn2 was depleted exhibited significantly elevated ENaC-mediated Na^+ transport compared to control siRNA treated cells, in the absence of aldosterone stimulation

(Fig. 6D). Conversely when Itsn2 expression was transiently increased (Fig. 6E) the ENaC-mediated Na^+ current was significantly reduced (Fig. 6F).

Discussion

There is currently little information about miRs and Na^+ regulation. Direct regulation of ENaC function by miRs was demonstrated by our group, and in a recent study the regulation of the serum glucocorticoid kinase (SGK1) was demonstrated to be altered by aldosterone-regulated miRs (Edinger et al., 2014; Jacobs et al., 2016). These studies suggest that miRs are capable of acting as intermediary components in the aldosterone signaling cascade (Edinger et al., 2014). Direct regulation of ENaC by miRs has been reported for miR-16 (Tamarapu Parthasarathy et al., 2012) and miR-7 (Qin et al., 2016) in alveolar epithelial cells and regulation of miR-101 and -199 by ENaC in endometrial cells (Sun et al., 2014). Neither of these reports focused on miR regulation by hormones, and none of these ENaC-targeting miRs were significantly altered in response to aldosterone in our microarray assays.

Studies have emerged investigating aldosterone regulation of Na^+ and K^+ transport in the kidney by miRs. miR-192 was identified as a possible regulator of K^+ secretion (Elvira-Matelot et al., 2010). Expression of this miR was inhibited in mice subject to K^+ load, salt depletion, or chronic aldosterone infusion. A confirmed target of miR-192 was the serine-threonine kinase, with no lysine (WNK1). From numerous studies, the role of L-WNK and the kidney specific form, KS-WNK have been elucidated and it is known that L-WNK1 is an important regulator of both K^+ and Na^+ transport (Lang et al., 2005; Yang et al., 2005; Subramanya et al., 2006; Wade et al., 2006; Huang and Kuo, 2007). Interestingly, we were unable to recapitulate this regulation of miR-192 in a mCCD cell line stimulated with aldosterone as part of our investigation into WNK1 regulation (Roy et al., 2015) and the reason for this discrepancy is unknown. miR regulation of the renal outer medullary potassium (ROMK) channel by miRs has been described. An increase in K^+ diet induced miR-194 expression. Intersectin 1 was determined to be a target of this regulated miR. An increase in miR-194 reduced Itsn1 expression and this in turn prevented the internalization of ROMK (Lin et al., 2014). This finding highlighted the possible role of Itsn2 in ENaC regulation even though the target UTRs are distinct for these two forms of Itsn.

The miR cluster family miR-23–24–27 has been implicated in regulation of aldosterone production, pointing to a possible feedback mechanism in vivo, but this has not been directly investigated (Robertson et al., 2013). It is likely that the genomic proximity of members of these miR clusters facilitate coordinated regulation, however, studies investigating these clusters have noted that cluster members can be regulated individually (Chhabra et al., 2010). Nevertheless, miR-27 has the most significant impact on ENaC-mediated Na^+ transport. No direct regulation of ENaC expression was predicted as none of the ENaC subunit UTRs in mouse contains canonical binding sites for the miR cluster members. However, several candidate targets were predicted and screened. We did not carry out validation of the all identified candidates as true miR-27 targets, but as mRNA expression of many of the targets decreased following overexpression of a miR-27 mimic, it is possible that a number of novel miR-27 targets have been identified in this study which will require additional investigation.

Similar to Itsn1, Itsn2 has a large number of reported functions, many of which center around their role in membrane trafficking and delivery/removal of proteins to and from the plasma membrane (Tsyba et al., 2011). Previous studies have noted differential protein interactions with Itsn1 compared to Itsn2 (Wong et al., 2012). As Itsns are large, multi-domain proteins, it suggests that they may have multiple functions in cells, including their more studied role in clathrin-mediated endocytosis. ENaC is known to interact with clathrin to co-ordinate endocytic retrieval from the apical membrane (Wang et al., 2006). As Itsn2 facilitates this endocytic event, the reduction in expression may delay ENaC removal from the apical surface. The mechanism underlying Itsn2 regulation of this process is under investigation. A model depicting the link between ENaC, Itsn2, and clathrin-mediated endocytosis is presented in Figure 7.

These studies provide an example of miR regulation in response to aldosterone in kidney epithelia. Given the large number of possible miR targets, some of which were screened in this study, it is likely that additional examples of miR regulation will emerge. Based on the screen of miR-27 targets it is also highly probable that the regulatory network controlled by aldosterone stimulation will be more substantial than currently appreciated. From this study and our previous work we note that changes in protein expression induced by alterations in miRs are likely to be more modest compared to the many fold changes reported for aldosterone induced/repressed proteins described to date. This is indeed the case for Itsn2. Nevertheless, smaller changes in a number of proteins all acting on a single target or pathway may be an effective way to facilitate dynamic homeostasis without the need for dramatic swings in protein expression. While we continue to uncover the roles of miR and their targets in normal renal physiology, an appreciation of miRs regulated by hormonal signaling cascades is emerging and could provide novel information of misregulation associated with non-homeostatic disease states.

Supplementary Material

Refer to Web version on PubMed Central for supplementary material.

Acknowledgments

Contract grant sponsor: NIH/NIDDK;

Contract grant numbers: R01DK102843, R00DK087922, R01DK103776, DK076169, P30CA047904.

Contract grant sponsor: American Heart Association;

Contract grant number: PRE25680068.

Contract grant sponsor: Carl W. Gottschalk Research Scholar.

Contract grant sponsor: American Society of Nephrology.

Contract grant sponsor: March of Dimes Basil O’Connor Starter Scholar Award.

Contract grant sponsor: NIDDK Diabetic Complications Consortium.

Contract grant sponsor: American Society of Nephrology.

Dr. Butterworth's laboratory is supported by funding from the NIH/NIDDK (DK102843) and the Carl W. Gottschalk Research Scholar Grant, from the American Society of Nephrology. Christine Klemens is supported by a pre-doctoral grant from the American Heart Association (PRE25680068). Dr. Ho's laboratory is supported by funding by an NIDDK R00DK087922, NIDDK R01DK103776, March of Dimes Basil O'Connor Starter Scholar Award and NIDDK Diabetic Complications Consortium grant DK076169. Dr. Yu Leng Phua is a George B. Rathmann Research Fellow supported by the Ben J. Lipps Research Fellowship Program from the American Society of Nephrology. This project used the University of Pittsburgh Cancer Institute shared resource facility (Cancer Genomics Facility) that is supported in part by award P30CA047904 (Dr LaFramboise).

Literature Cited

Abbott AL, Alvarez-Saavedra E, Miska EA, Lau NC, Bartel DP, Horvitz HR, Ambros V. The let-7 MicroRNA family members mir-48, mir-84, and mir-241 function together to regulate developmental timing in caenorhabditis elegans. Dev Cell. 2005; 9:403–414. [PubMed: 16139228]

Abdelmohsen K, Kim MM, Srikantan S, Mercken EM, Brennan SE, Wilson GM, Cabo R, Gorospe M. MiR-519 suppresses tumor growth by reducing HuR levels. Cell Cycle. 2010; 9:1354–1359. [PubMed: 20305372]

Agarwal V, Bell GW, Nam JW, Bartel DP. Predicting effective microRNA target sites in mammalian mRNAs. eLife. 2015; 4:e05005.

Agrawal R, Tran U, Wessely O. The miR-30 miRNA family regulates xenopus pronephros development and targets the transcription factor Xlim1/Lhx1. Development. 2009; 136:3927–3936. [PubMed: 19906860]

Asher C, Wald H, Rossier BC, Garty H. Aldosterone-induced increase in the abundance of Na+ channel subunits. Am J Physiol Cell Physiol. 1996; 271:C605–C611.

Butterworth MB. MicroRNAs and the regulation of aldosterone signaling in the kidney. Am J Physiol Cell Physiol. 2015; 308:C521–C527. [PubMed: 25673770]

Campese VM, Park J. The kidney and hypertension: Over 70 years of research. J Nephrol. 2006; 19:691–698. [PubMed: 17173239]

Chhabra R, Dubey R, Saini N. Cooperative and individualistic functions of the microRNAs in the miR-23a~27a~24-2 cluster and its implication in human diseases. Mol Cancer. 2010; 9:232. [PubMed: 20815877]

Chu JY, Sims-Lucas S, Bushnell DS, Bodnar AJ, Kreidberg JA, Ho J. Dicer function is required in the metanephric mesenchyme for early kidney development. Am J Physiol Renal Physiol. 2014; 306:F764–F772. [PubMed: 24500693]

Edinger RS, Bertrand CA, Rondandino C, Apodaca GA, Johnson JP, Butterworth MB. The epithelial sodium channel (ENaC) establishes a trafficking vesicle pool responsible for its regulation. PLoS ONE. 2012; 7:e46593. [PubMed: 23029554]

Edinger RS, Coronnello C, Bodnar AJ, Labarca M, Bhalla V, LaFramboise WA, Benos PV, Ho J, Johnson JP, Butterworth MB. Aldosterone regulates microRNAs in the cortical collecting duct to alter sodium transport. J Am Soc Nephrol. 2014; 25:2445–2457. [PubMed: 24744440]

Elvira-Matelot E, Zhou XO, Farman N, Beaurain G, Henrion-Caude A, Hadchouel J, Jeunemaitre X. Regulation of WNK1 expression by miR-192 and aldosterone. J Am Soc Nephrol. 2010; 21:1724–1731. [PubMed: 20813867]

Farh KK, Grimson A, Jan C, Lewis BP, Johnston WK, Lim LP, Burge CB, Bartel DP. The widespread impact of mammalian MicroRNAs on mRNA repression and evolution. Science. 2005; 310:1817–1821. [PubMed: 16308420]

Harvey SJ, Jarad G, Cunningham J, Goldberg S, Schermer B, Harfe BD, McManus MT, Benzing T, Miner JH. Podocyte-specific deletion of dicer alters cytoskeletal dynamics and causes glomerular disease. J Am Soc Nephrol. 2008; 19:2150–2158. [PubMed: 18776121]

Ho J, Ng KH, Rosen S, Dostal A, Gregory RI, Kreidberg JA. Podocyte-specific loss of functional microRNAs leads to rapid glomerular and tubular injury. J Am Soc Nephrol. 2008; 19:2069–2075. [PubMed: 18832437]

Ho J, Pandey P, Schatton T, Sims-Lucas S, Khalid M, Frank MH, Hartwig S, Kreidberg JA. The pro-apoptotic protein bim is a microRNA target in kidney progenitors. J Am Soc Nephrol. 2011; 22:1053–1063. [PubMed: 21546576]

Hsueh WA, Wyne K. Renin-Angiotensin-aldosterone system in diabetes and hypertension. J Clin Hypertens. 2011; 13:224–237.

Huang CL, Kuo E. Mechanisms of disease: WNK-ing at the mechanism of salt-sensitive hypertension. Nat Clin Pract Nephrol. 2007; 3:623–630. [PubMed: 17957199]

Jacobs ME, Kathpalia PP, Chen Y, Thomas SV, Noonan EJ, Pao AC. SGK1 regulation by miR-466g in cortical collecting duct cells. Am J Physiol Renal Physiol Renal Physiol. 2016; 310:F1251–F1257.

Kato M, Putta S, Wang M, Yuan H, Lanting L, Nair I, Gunn A, Nakagawa Y, Shimano H, Todorov I, Rossi JJ, Natarajan R. TGF-beta activates Akt kinase through a microRNA-dependent amplifying circuit targeting PTEN. Nat Cell Biol. 2009; 11:881–889. [PubMed: 19543271]

Kato M, Wang L, Putta S, Wang M, Yuan H, Sun G, Lanting L, Todorov I, Rossi JJ, Natarajan R. Post-transcriptional up-regulation of Tsc-22 by Ybx1, a target of miR-216a, mediates TGF-{beta}-induced collagen expression in kidney cells. J Biol Chem. 2010; 285:34004–34015. [PubMed: 20713358]

Kato M, Zhang J, Wang M, Lanting L, Yuan H, Rossi JJ, Natarajan R. MicroRNA-192 in diabetic kidney glomeruli and its function in TGF-beta-induced collagen expression via inhibition of E-box repressors. Proc Natl Acad Sci USA. 2007; 104:3432–3437. [PubMed: 17360662]

Krupa A, Jenkins R, Luo DD, Lewis A, Phillips A, Fraser D. Loss of MicroRNA-192 promotes fibrogenesis in diabetic nephropathy. J Am Soc Nephrol. 2010; 21:438–447. [PubMed: 20056746]

Landgraf P, Rusu M, Sheridan R, Sewer A, Iovino N, Aravin A, Pfeffer S, Rice A, Kamphorst AO, Landthaler M, Lin C, Socci ND, Hermida L, Fulci V, Chiaretti S, Foa R, Schliwka J, Fuchs U, Novosel A, Muller RU, Schermer B, Bissels U, Inman J, Phan Q, Chien M, Weir DB, Choksi R, De Vita G, Frezzetti D, Trompeter HI, Hornung V, Teng G, Hartmann G, Palkovits M, Di Lauro R, Wernet P, Macino G, Rogler CE, Nagle JW, Ju J, Papavasiliou FN, Benzing T, Lichter P, Tam W, Brownstein MJ, Bosio A, Borkhardt A, Russo JJ, Sander C, Zavolan M, Tuschl T. A mammalian microRNA expression atlas based on small RNA library sequencing. Cell. 2007; 129:1401–1414. [PubMed: 17604727]

Lang F, Capasso G, Schwab M, Waldegger S. Renal tubular transport and the genetic basis of hypertensive disease. Clin Exp Nephrol. 2005; 9:91–99. [PubMed: 15980941]

Lewis BP, Burge CB, Bartel DP. Conserved seed pairing, often flanked by adenosines, indicates that thousands of human genes are microRNA targets. Cell. 2005; 120:15–20. [PubMed: 15652477]

Lewis BP, Shih IH, Jones-Rhoades MW, Bartel DP, Burge CB. Prediction of mammalian microRNA targets. Cell. 2003; 115:787–798. [PubMed: 14697198]

Lin DH, Yue P, Zhang C, Wang WH. MicroRNA-194 (miR-194) regulates ROMK channel activity by targeting intersectin 1. Am J Physiol Renal Physiol. 2014; 306:F53–F60. [PubMed: 24197061]

Loffing J, Summa V, Zecevic M, Verrey F. Mediators of aldosterone action in the renal tubule. Curr Opin Nephrol Hypertens. 2001; 10:667–675. [PubMed: 11496063]

Lorenzen JM, Kielstein JT, Hafer C, Gupta SK, Kumpers P, Faulhaber-Walter R, Haller H, Fliser D, Thum T. Circulating miR-210 predicts survival in critically ill patients with acute kidney injury. Clin J Am Soc Nephrol. 2011; 6:1540–1546. [PubMed: 21700819]

Martel JA, Michael D, Fejes-Toth G, Naray-Fejes-Toth A. Melanophilin, a novel aldosterone-induced gene in mouse cortical collecting duct cells. Am J Physiol Renal Physiol. 2007; 293:F904–F913. [PubMed: 17609287]

McCormick JA, Bhalla V, Pao AC, Pearce D. SGK1: A rapid aldosterone-induced regulator of renal sodium reabsorption. Physiology (Bethesda). 2005; 20:134–139. [PubMed: 15772302]

Mladinov D, Liu Y, Mattson DL, Liang M. MicroRNAs contribute to the maintenance of cell-type-specific physiological characteristics: MiR-192 targets Na+/K+-ATPase beta1. Nucleic Acids Res. 2013; 41:1273–1283. [PubMed: 23221637]

Muller OG, Parnova RG, Centeno G, Rossier BC, Firsov D, Horisberger JD. Mineralocorticoid effects in the kidney: Correlation between alphaENaC, GILZ, and Sgk-1 mRNA expression and urinary excretion of Na+ and K+ J Am Soc Nephrol. 2003; 14:1107–1115. [PubMed: 12707381]

Nesterov V, Dahlmann A, Krueger B, Bertog M, Loffing J, Korbmacher C. Aldosterone-dependent and -independent regulation of the epithelial sodium channel (ENaC) in mouse distal nephron. Am J Physiol Renal Physiol. 2012; 303:F1289–F1299. [PubMed: 22933298]

Pacha J, Frindt G, Antonian L, Silver RB, Palmer LG. Regulation of Na channels of the rat cortical collecting tubule by aldosterone. J Gen Physiol. 1993; 102:25–42. [PubMed: 8397276]

Pandey P, Brors B, Srivastava PK, Bott A, Boehn SN, Groene HJ, Gretz N. Microarray-based approach identifies microRNAs and their target functional patterns in polycystic kidney disease. BMC Genomics. 2008; 9:624. [PubMed: 19102782]

Pandey P, Qin S, Ho J, Zhou J, Kreidberg JA. Systems biology approach to identify transcriptome reprogramming and candidate microRNA targets during the progression of polycystic kidney disease. BMC Syst Biol. 2011; 5:56. [PubMed: 21518438]

Pastorelli LM, Wells S, Fray M, Smith A, Hough T, Harfe BD, McManus MT, Smith L, Woolf AS, Cheeseman M, Greenfield A. Genetic analyses reveal a requirement for Dicer1 in the mouse urogenital tract. Mamm Genome. 2009; 20:140–151. [PubMed: 19169742]

Pechstein A, Bacetic J, Vahedi-Faridi A, Gromova K, Sundborger A, Tomlin N, Krainer G, Vorontsova O, Schafer JG, Owe SG, Cousin MA, Saenger W, Shupliakov O, Haucke V. Regulation of synaptic vesicle recycling by complex formation between intersectin 1 and the clathrin adaptor complex AP2. Proc Natl Acad Sci USA. 2010; 107:4206–4211. [PubMed: 20160082]

Pouly D, Debonneville A, Ruffieux-Daidie D, Maillard M, Abriel H, Loffing J, Staub O. Mice carrying ubiquitin-specific protease 2 (Usp2) gene inactivation maintain normal sodium balance and blood pressure. Am J Physiol Renal Physiol. 2013; 305:F21–F30. [PubMed: 23552861]

Powers MP, Alvarez K, Kim HJ, Monzon FA. Molecular classification of adult renal epithelial neoplasms using microRNA expression and virtual karyotyping. Diagn Pathol. 2011; 20:63–70.

Qi W, Li H, Cai XH, Gu JQ, Meng J, Xie HQ, Zhang JL, Chen J, Jin XG, Tang Q, Hao Y, Gao Y, Wen AQ, Xue XY, Gao Smith F, Jin SW. Lipoxin A4 activates alveolar epithelial sodium channel gamma via the microRNA-21/PTEN/AKT pathway in lipopolysaccharide-induced inflammatory lung injury. Lab Invest. 2015; 95:1258–1268. [PubMed: 26302186]

Qin K, Zhong X, Wang D. MicroRNA-7-5p regulates human alveolar epithelial sodium channels by targeting the mTORC2/SGK-1 signaling pathway. Exp Lung Res. 2016; 42:237–244. [PubMed: 27331901]

Qin W, Chung AC, Huang XR, Meng XM, Hui DS, Yu CM, Sung JJ, Lan HY. TGF-beta/Smad3 signaling promotes renal fibrosis by inhibiting miR-29. J Am Soc Nephrol. 2011; 22:1462–1474. [PubMed: 21784902]

Robertson S, MacKenzie SM, Alvarez-Madrazo S, Diver LA, Lin J, Stewart PM, Fraser R, Connell JM, Davies E. MicroRNA-24 is a novel regulator of aldosterone and cortisol production in the human adrenal cortex. Hypertension. 2013; 62:572–578. [PubMed: 23836801]

Roy A, Al-Qusairi L, Donnelly BF, Ronzaud C, Marciszyn AL, Gong F, Chang YP, Butterworth MB, Pastor-Soler NM, Hallows KR, Staub O, Subramanya AR. Alternatively spliced proline-rich cassettes link WNK1 to aldosterone action. J Clin Invest. 2015; 125:3433–3448. [PubMed: 26241057]

Sequeira-Lopez ML, Weatherford ET, Borges GR, Monteagudo MC, Pentz ES, Harfe BD, Carretero O, Sigmund CD, Gomez RA. The microRNA-processing enzyme dicer maintains juxtaglomerular cells. J Am Soc Nephrol. 2010; 21:460–467. [PubMed: 20056748]

Shi S, Yu L, Chiu C, Sun Y, Chen J, Khitrov G, Merkenschlager M, Holzman LB, Zhang W, Mundel P, Bottinger EP. Podocyte-selective deletion of dicer induces proteinuria and glomerulosclerosis. J Am Soc Nephrol. 2008; 19:2159–2169. [PubMed: 18776119]

Sober S, Laan M, Annilo T. MicroRNAs miR-124 and miR-135a are potential regulators of the mineralocorticoid receptor gene (NR3C2) expression. Biochem Biophys Res Commun. 2010; 391:727–732. [PubMed: 19944075]

Spindler B, Mastroberardino L, Custer M, Verrey F. Characterization of early aldosterone-induced RNAs identified in A6 kidney epithelia. Pflugers Archiv. 1997; 434:323–331. [PubMed: 9178633]

Subramanya AR, Yang CL, McCormick JA, Ellison DH. WNK kinases regulate sodium chloride and potassium transport by the aldosterone-sensitive distal nephron. Kidney Int. 2006; 70:630–634. [PubMed: 16820787]

Sun X, Ruan YC, Guo J, Chen H, Tsang LL, Zhang X, Jiang X, Chan HC. Regulation of miR-101/miR-199a-3p by the epithelial sodium channel during embryo implantation: Involvement of CREB phosphorylation. Reproduction. 2014; 148:559–568. [PubMed: 25187622]

Tamarapu Parthasarathy P, Galam L, Huynh B, Yunus A, Abuelenen T, Castillo A, Kollongod Ramanathan G, Cox R Jr, Kolliputi N. MicroRNA 16 modulates epithelial sodium channel in human alveolar epithelial cells. Biochem Biophys Res Commun. 2012; 426:203–208. [PubMed: 22940131]

Tsyba L, Nikolaienko O, Dergai O, Dergai M, Novokhatska O, Skrypkina I, Rynditch A. Intersectin multidomain adaptor proteins: Regulation of functional diversity. Gene. 2011; 473:67–75. [PubMed: 21145950]

Verrey F. Transcriptional control of sodium transport in tight epithelial by adrenal steroids. J Memb Biol. 1995; 144:93–110.

Verrey F, Fakitsas P, Adam G, Staub O. Early transcriptional control of ENaC (de) ubiquitylation by aldosterone. Kidney Int. 2007; 73:691–696. [PubMed: 18094676]

Wade JB, Fang L, Liu J, Li D, Yang CL, Subramanya AR, Maouyo D, Mason A, Ellison DH, Welling PA. WNK1 kinase isoform switch regulates renal potassium excretion. Proc Natl Acad Sci USA. 2006; 103:8558–8563. [PubMed: 16709664]

Wang H, Traub LM, Weixel KM, Hawryluk MJ, Shah N, Edinger RS, Perry CJ, Kester L, Butterworth MB, Peters KW, Kleyman TR, Frizzell RA, Johnson JP. Clathrin-mediated endocytosis of the epithelial sodium channel. Role of epsin. J Biol Chem. 2006; 281:14129–14135. [PubMed: 16574660]

Wei Q, Bhatt K, He HZ, Mi QS, Haase VH, Dong Z. Targeted deletion of Dicer from proximal tubules protects against renal ischemia-reperfusion injury. J Am Soc Nephrol. 2010; 21:756–761. [PubMed: 20360310]

Wei Q, Mi QS, Dong Z. The regulation and function of microRNAs in kidney diseases. IUBMB Life. 2013; 65:602–614. [PubMed: 23794512]

Wong KA, Wilson J, Russo A, Wang L, Okur MN, Wang X, Martin NP, Scappini E, Carnegie GK, O'Bryan JP. Intersectin (ITSN) family of scaffolds function as molecular hubs in protein interaction networks. PLoS ONE. 2012; 7:e36023. [PubMed: 22558309]

Wong N, Wang X. MiRDB: An online resource for microRNA target prediction and functional annotations. Nucleic Acids Res. 2015; 43:D146–D152. [PubMed: 25378301]

Yang CL, Zhu X, Wang Z, Subramanya AR, Ellison DH. Mechanisms of WNK1 and WNK4 interaction in the regulation of thiazide-sensitive NaCl cotransport. J Clin Invest. 2005; 115:1379–1387. [PubMed: 15841204]

Zhong X, Chung AC, Chen HY, Meng XM, Lan HY. Smad3-mediated upregulation of miR-21 promotes renal fibrosis. J Am Soc Nephrol. 2011; 22:1668–1681. [PubMed: 21852586]

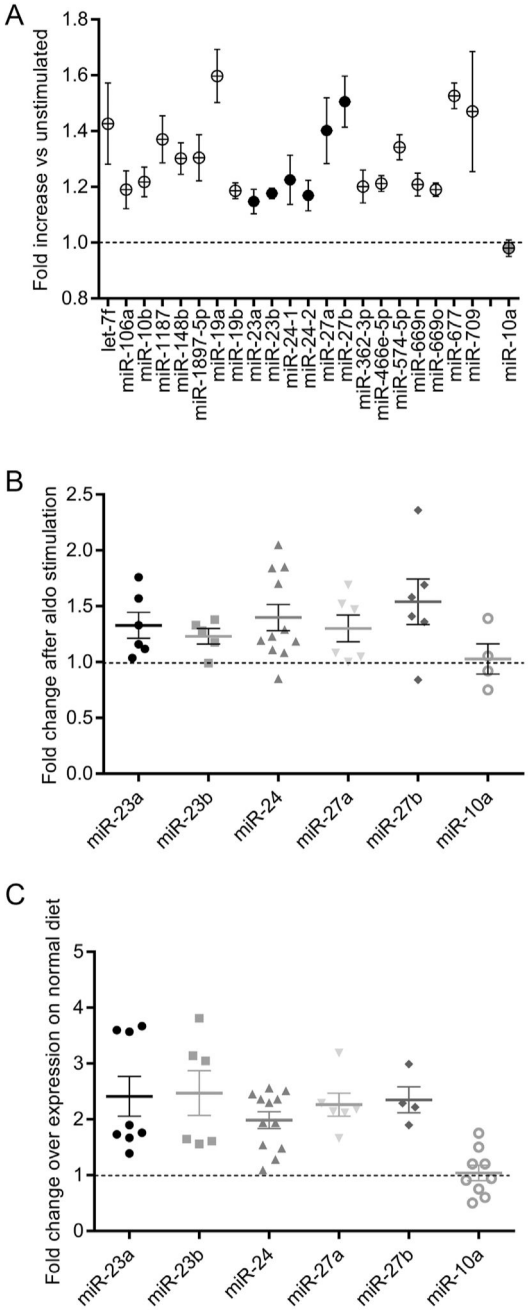

Fig. 1.

Aldosterone upregulates miRs in the CCD. (A) Summary of microarray analysis profiling mouse miRs in mCCD cells with or without aldosterone stimulation (50 nM, 24 h). Abundantly expressed miRs that were significantly upregulated are plotted as a fold increase from unstimulated levels (mean ±SEM, n = 5 arrays). Expression of miR-10a was not significantly altered in response to aldosterone and served as control for subsequent investigations. (B) Quantitative PCR analysis of selected miRs in the MIRC11 and MIRC22 clusters to verify upregulation after aldosterone (50 nM, 24 h) as identified by microarrays in A. Relative miR expression is plotted as a fold change from unstimulated cells (mean

±SEM, n≥4). Expression of all miRs, except miR-10a are significantly >1 (unstimulated) (P <0.05). (C) Relative expression of miRs in isolated CCD epithelial cells from mice fed low Na^+ diets (to induce aldosterone stimulation) expressed as a fold change from miR expression in cells isolated from mice on normal Na^+ diet (mean ±SEM, n≥4). Expression of all miRs, except miR-10a are significantly >1 (normal diet) (P <0.05).

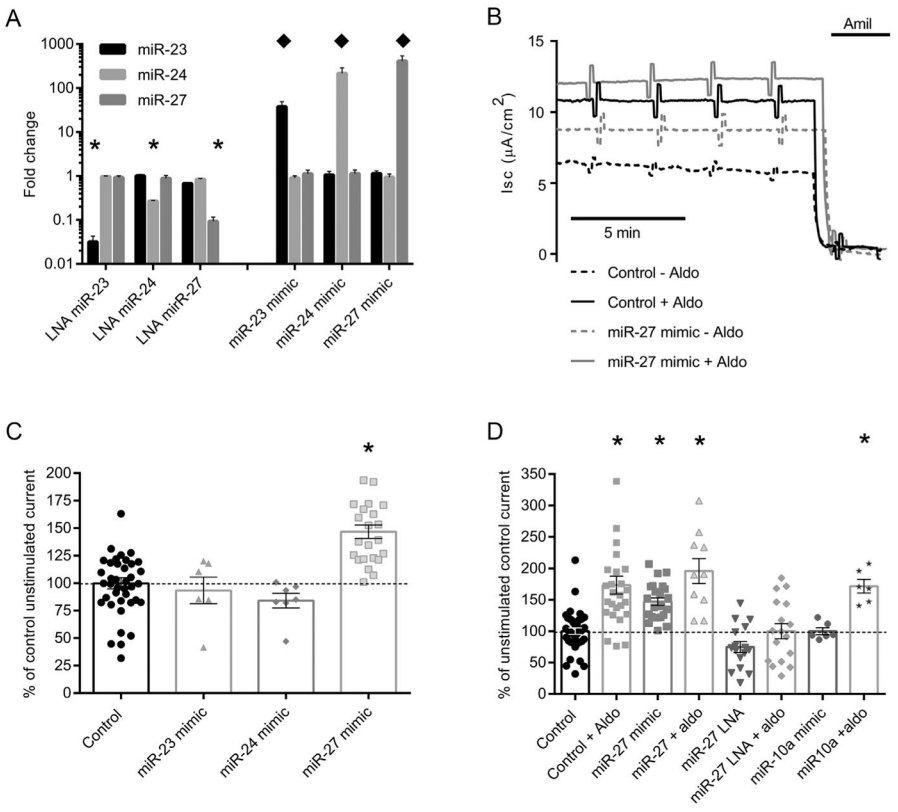

Fig. 2.

Altering miR-27 expression regulates ENaC activity. (A) The specific depletion (LNA) or overexpression (mimic) of miRs was confirmed by qPCR for miRs-23,24,27 in mCCD cells. Cells were transfected with a specific miR inhibitor (LNA) (50 nM), or miR mimic (50 nM) and miR expression for all miRs in the cluster was normalized to control transfected mCCD cells. A significant reduction in targeted miRs was confirmed for LNA transfected cells (* = P <0.01) with no off-target alteration in other cluster family members. Likewise, mimic overexpression did not significantly alter endogenous miR expression but a significantly greater level of mature miR (◆ = P <0.01) was detected by qPCR (mean ±SEM, n = 3). (B) Representative traces of short-circuit current measurements from mCCD cells mounted in modified Ussing chambers. Cells were transfected with miR-27 mimic (50 nM) and stimulated with aldosterone (50 nM). (C) Summary of the amiloride-sensitive short circuit current measurements similar to those presented in (B) normalized to unstimulated control siRNA transfected mCCD cells. A significant increase in ENaC current (* = P <0.001) was only observed in miR-27 overexpressing mCCDs (mean ±SEM). (D) The mCCD cell response to aldosterone is expressed as a pertentage of control (unstimulated) amiloride-sensitive current. Overexpression of miR-27 mimics significantly increased basal (unstimulated) and aldosterone stimulated current (* = P <0.01) compared to control, but there was no significant difference between the aldosterone responses in control versus miR-27 overexpressing cells. Inhibiting miR-27 by LNA transfection significantly reduced basal (unstimulated) ENaC currents (P <0.02) and blunted the aldosterone stimulation compared to control transfected cells (ND compared to control unstimulated). As a control,

there was no significant difference in either the basal or aldosterone stimulated current in miR-10a overexpressing mCCD cells (mean ±SEM, n≥6).

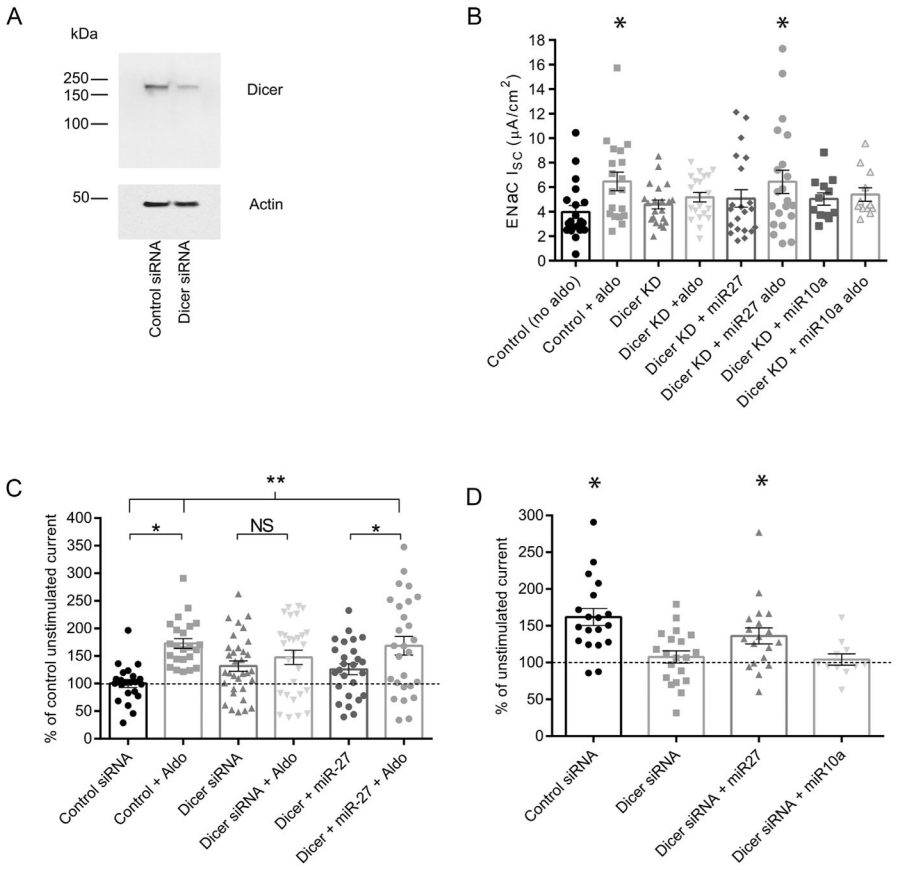

Fig. 3.

Dicer depletion inhibits aldosterone signaling, which is restored with miR-27 overexpression. (A) Dicer1 expression was depleted using siRNA, and verified by Western blot. Densitometric analysis of Dicer depletion normalized to actin produced a mean decrease of 63.1 ± 23.2% compared to control siRNA transfected CCD cells (n = 3). (B) Amiloride-sensitive I_{SC} measurements from mCCD cells stimulated with 10 nM aldosterone (24 h). Dicer depleted cells failed to significantly respond to aldosterone compared to control siRNA transfected cells. Dicer depleted mCCD cells co-transfected with miR-27a mimic produced a significant increase (* = P <0.05) in I_{SC} with aldosterone stimulation, which was not observed in control Dicer depleted cells overexpressing miR-10a. (C) ENaC-mediated I_{SC} normalized to the unstimulated I_{SC} from each experimental replicate (N = 4, n = 10–20). A significant increase in both baseline and aldosterone stimulated I_{SC} over control, unstimulated cells was observed for all Dicer depleted cells (**indicates significant increase over control siRNA, P <0.05). A significant I_{SC} response to aldosterone stimulation was observed in control and Dicer depleted cells overexpressing miR-27 (*indicates significant difference P <0.05). No significant increase (above the elevated baseline) was observed in Dicer depleted cells stimulated with aldosterone (NS). (D) Percentage increase in ENaC-mediated I_{SC} following aldosterone stimulation, normalized to the unstimulated I_{SC} from each experimental replicate (N = 6, n = 11–20) (*indicates significant increase P <0.05).

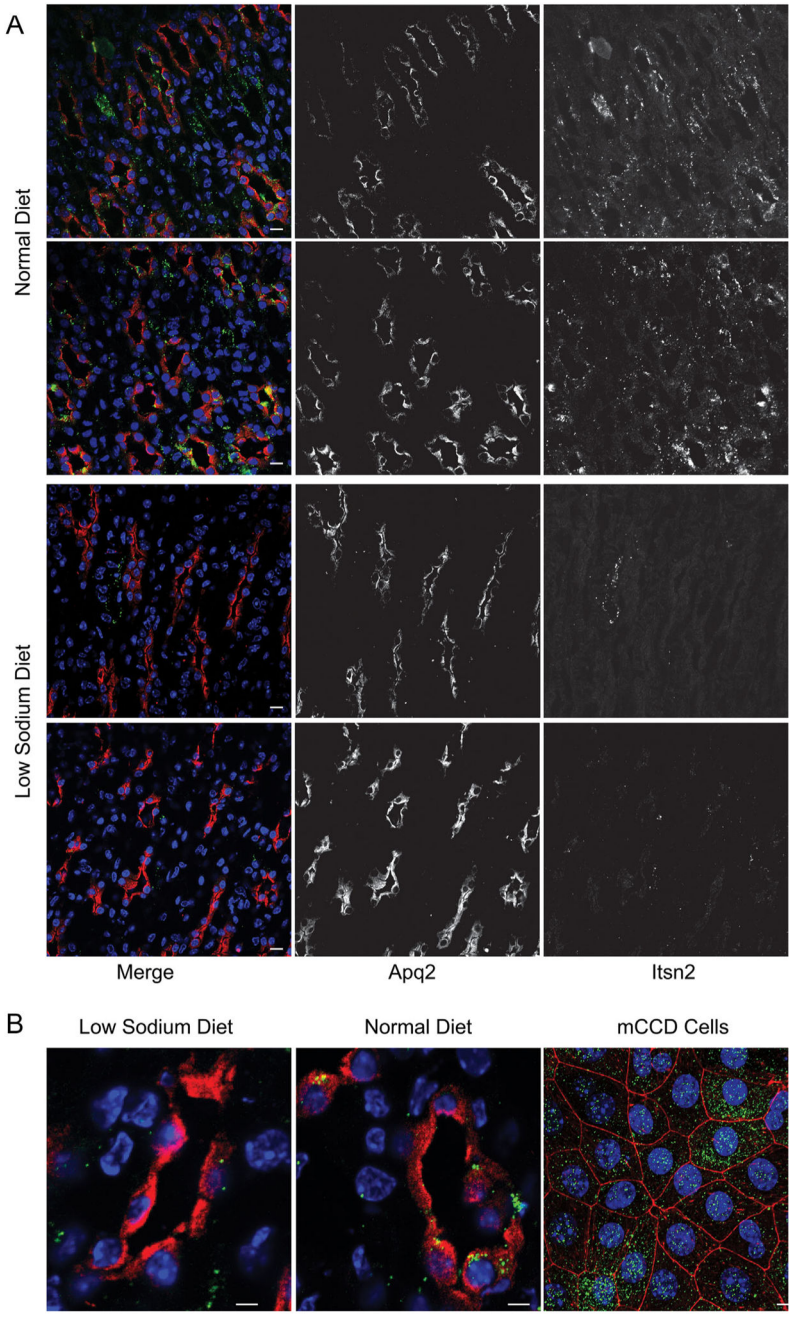

Fig. 4.

Intersectin 2 is expressed in kidney distal nephron epithelial cells. (A) Endogenous expression of Itsn2 (green in left and right parts) in mouse kidney sections taken from mice on normal (top 2 parts) and low Na^+ diets (lower 2 part) using the goat antibody. Principal cells of the CCD were identified by co-labeling with anti-Aqp2 antibodies (red in composite image and middle parts). (B) A higher power magnification in Aqp2-positive (red) kidney tubules under normal and low Na^+ diet. Itsn2 expression (green, using the goat antibody) in mCCD cells cultured on filters exhibits a punctate/vesicular distribution (right part). Cortical

actin counterstaining (red) using phalloidin outlines the cell periphery. All nuclei are counterstained in blue. Scale bar represents 5 μm.

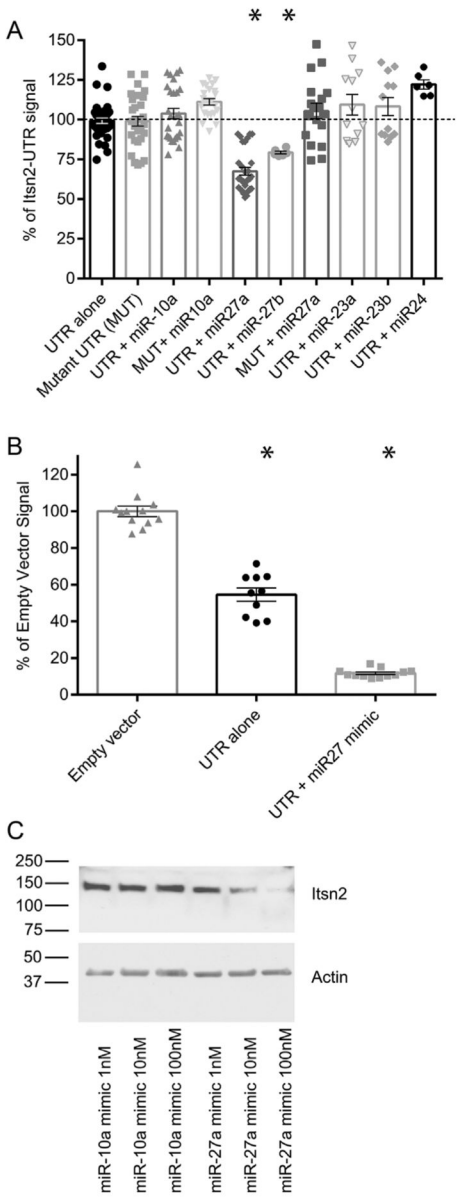

Fig. 5.

miR-27 binds to the 3′-UTR of Intersectin 2 and reduces protein expression. (A) Normalized luciferase signal from HEK293 cells transfected with a dual luciferase reporter plasmid expressing a wild type (wt) 3′-UTR of Itsn2 or 3′-UTR Itsn2 mutant (MUT) lacking the miR-27 seed sequence. Cells were transfected with the 3′-UTR reporter alone or reporter with miR mimics as indicated. A significant reduction (* = P <0.01) in luciferase signal was detected only in the wt Itsn2 3′-UTR transfected with miR27a or miR27b mimics, with no reduction in luciferase signal for any of the other cluster family members or miR-10a as a control. The specific depression in luciferase was restored in the MUT reporter verifying specific binding of miR-27 to the predicted seed site. (B) The same wt reporter construct was transfected into mCCD cells alone, or in the presence of miR-27a mimic. The normalized luciferase signal was significantly decreased compared to the blank reporter

plasmid. This signal was further reduced when cells were co-transfected with the miR-27 mimic (* = P <0.01). (C) Representative Western blot (using the goat antibody) to show whole cell protein expression of Itsn2 in mCCD cells transfected with increasing miR mimic concentrations for miR-10a (control) or miR-27 mimics (as indicated) after 24 h. Itsn2 protein expression decreased with increasing Itsn2 concentration and was significantly lower than control transfected mCCD cells at 100 nM (92 ± 24% for miR-10a and 33 ± 21% for miR-27a compared to 1 nM transfection, n = 3).

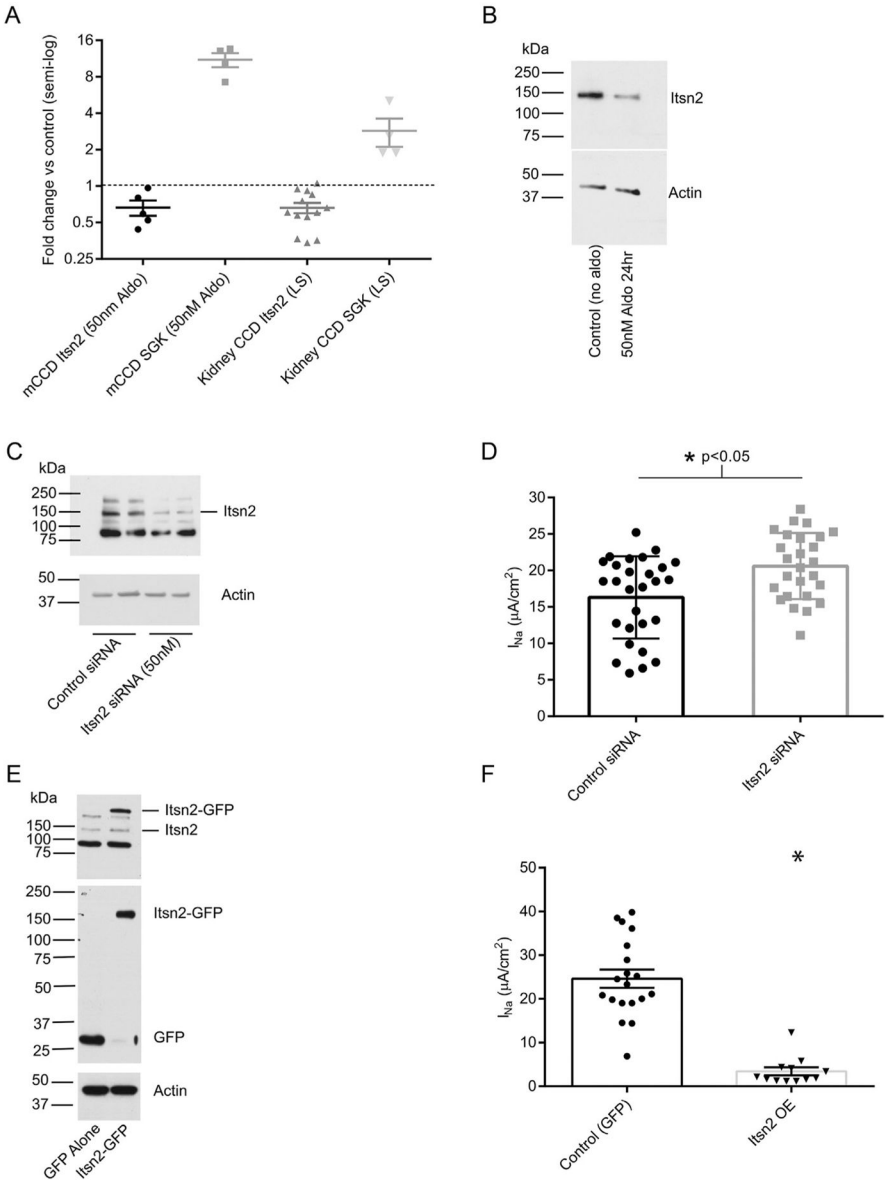

Fig. 6.

Itsn2 mRNA and protein expression decreases with aldosterone stimulation and changes in Itsn2 expression regulate ENaC activity. (A) Quantitative RT-PCR analysis of Itsn2 mRNA expression in mCCD cells following aldosterone stimulation (50 nM, 24 h) or CCD cells isolated from mouse kidneys on low Na^+ diets. A significant reduction in Itsn2 mRNA levels was measured in both in vitro and ex vivo samples (P <0.03). As a control, expression of SGK1 a known aldosterone-induced protein was significantly increased in both systems to confirm aldosterone signaling. (B) Itsn2 protein expression as determined by Western blotting (using the goat antibody) was significantly reduced in mCCD cells following aldosterone stimulation (50 nM, 24 h). Quantification of n = 4 similar experiments produced a mean reduction to 43.2 ± 6.2% of control (unstimulated) expression. (C) Itsn2 expression was depleted in mCCD cells using siRNA as determined by Western blotting using the

rabbit antibody. A significant reduction in Itsn2 protein (71.4 ± 15.2% decrease, n = 3) was achieved with 50 nM siRNA. (D) Itsn2 depleted cells had a significantly greater amiloride-sensitive I_{SC} relative to control siRNA transfected cells in the absence of aldosterone stimulation or serum supplementation. (E) Overexpression of GFP-tagged Itsn2 in mCCD cells was confirmed by Western blot, using both an anti-Intersectin-2 antibody (rabbit, top part) and anti-GFP antibody (middle part). (F) Amiloride-sensitive I_{SC} was significantly reduced in mCCD cells over expressing Itsn2 relative to control, GFP-alone, expressing cells.

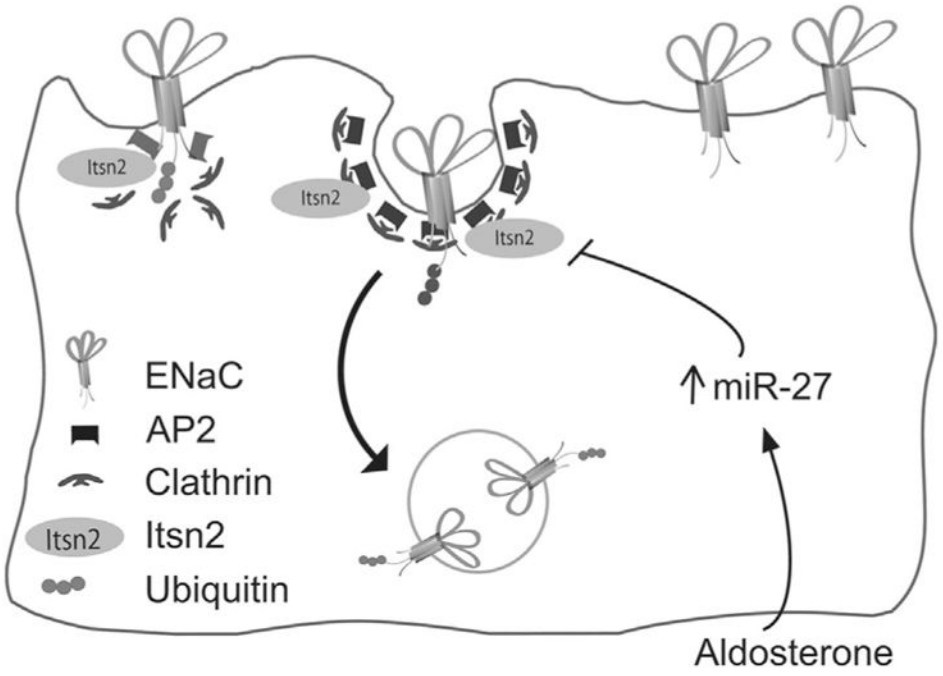

Fig. 7.

Schematic model depicting the interaction between Itsn2 and ENaC in clathrin-mediated endocytosis from the apical surface. Aldosterone would increase miR-27 expression and decrease Itsn2 abundance resulting in a deficiency in ENaC removal from the surface.

TABLE 1

List of predicted miR-27a targets screened for regulation of mRNA expression following miR-27 mimic over-expression (50 nM, 24 h) or aldosterone stimulation (50 nM, 24 h) by qRT-PCR

Gene target	Change after miR-27 mimic over-expression	Change after aldosterone stimulation
Itsn2	−	−
Cds1	−	−
Dcun1d4	−	−
Pparg	ND	−
Gcc2	−	−
trim23	−	−
Ube2n	−	−
Pkia	+	NC
Nr2f6	−	−
Nr5a2	NC	−
Sik1	+	−
Grb2	NC	NC

Relative change in expression is characterized as +, up-regulation; −, down-regulation; NC, no significant change; or ND, not determined. Primer sequences are listed in the supplementary data Table S1.